Reply to the comments by Referee #2

We thank the reviewer for the comments and suggestions to improve our manuscript. Below is our point-by-point response to these comments. The reviewer's comments are in italics, our responses are in normal font, and manuscript revisions are in blue.

General comments

Comment 1*:*

The authors briefly summarized the subgrid surface heat flux scheme initially proposed by Sun et al. (2021) and specifically introduced the modified version. These two stochastic sampling models actually introduce the uncertainties into the land-atmosphere coupling process other than, as the authors claimed, represent the realistic surface heat flux partitioning. How does the model deal with the surface energy balance closure in accompany with the imposed heat flux partitioning? On the assumption of normal distribution of the surface heat fluxes, how many land grid cells are subject to that normal distribution if the purpose of this study is to parameterize the realistic surface heat fluxes? And to what extent the other "abnormal" grid cells can play roles in impacting the simulated climate? I understand that it may be difficult to address these points at one time, but it will benefit the readers if the authors can provide some advantages and disadvantages of Sun's approach and the modified approach in the text.

Reply: Thanks for the insightful comments. The surface energy balance closure **at the grid scale** is not affected by both the stochastic sampling method and the follow-up collocation of the sampled sensible and latent heat fluxes according to their correlation coefficient **at the subgrid scale**. **Note that the surface energy balance has been closed at the grid scale in the default land-atmosphere coupling way.** Therefore, the stochastic sampling at the subgrid scale based on the truncated normal distributions with the mean values equal to the default grid averages calculated by the weighted fluxes on each PFT within the grid cell can assure the grid-scale surface energy balance closed as well in the long-term statistics, although at a given time step this might be broken up. This is confirmed by Fig. R1 where the distributions of sampled sensible heat fluxes highly resemble the realistic distributions of sensible heat fluxes within the given grid cells in the long-term statistics. As a result, their grid averages are comparable. This feature is not affected by the follow-up collocation of the sampled sensible and latent heat fluxes because this process does not alter the sampled values just arranging them in a given sequence. We clarified this in Lines 110-114 in the revision:

"Note that the surface energy balance closure at the grid scale is not affected by the stochastic sampling method. The surface energy balance has been closed at the grid scale in the default land-atmosphere coupling way. Therefore, the stochastic sampling at the subgrid scale based on the truncated normal distributions with the mean values equal to the default grid averages calculated by the weighted fluxes on each PFT within

the grid cell (Fig. 1) can assure the grid-scale surface energy balance closed as well in the long-term statistics, although at a given time step this might be broken up."

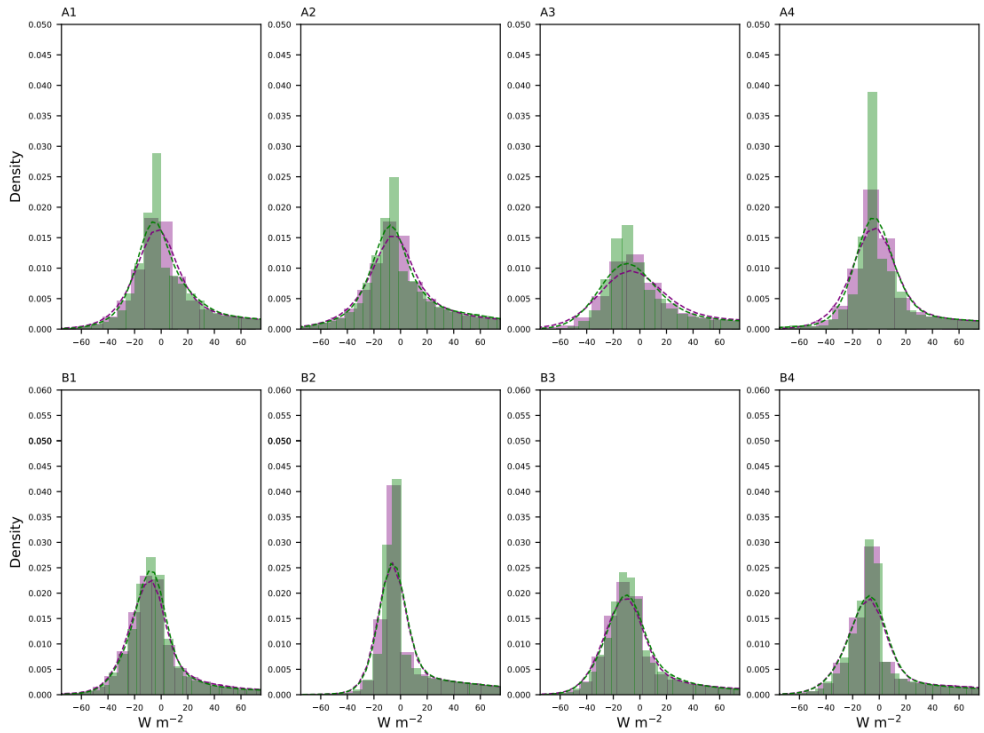

Figure R1. The histogram and gaussian kernel density estimate (KDE) (dashed line) of the sensible heat fluxes at the PFT in the eight grid cells with 16 (top row) and 8 (bottom row) PFTs, respectively. Green histograms and KDE estimates show the distribution of realistic sensible heat fluxes at the PFT within each grid cell while purple histograms and KDE estimates are for the distribution of sampled sensible heat fluxes based on the assumed normal distribution.

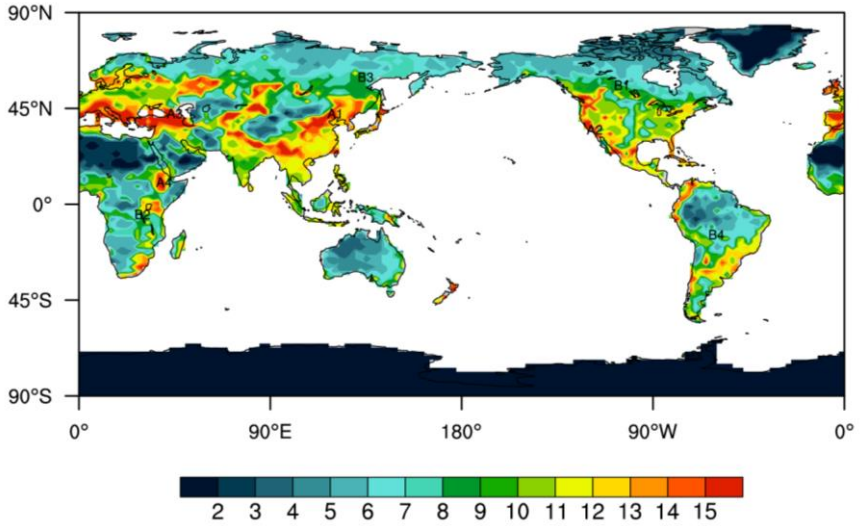

Figure R2. Number of PFTs in each grid cell. "A*" and "B*" denote the grid cell with 16 and 8 PFTs, respectively.

To verify the validity of the assumed normal distribution, we randomly selected land grids where the subgrid PFTs are as many as possible because, with fewer subgrid PFTs within the grid cell, the diversity of the realistic fluxes (associated with extreme conditions) reduces. Figure R1 shows the results over those grid cells with the maximum number of PFTs (i.e., 16) and the half (i.e., 8) both covering climate regimes as many as possible (Fig. R2). We can see that no matter for 16 PFTs or 8, the distributions of sampled sensible heat fluxes highly resemble the realistic distributions within the given grid cells in the long-term statistics. Therefore, the assumed normal distribution works well and thus the sampled samples can represent the realistic features for climate simulation. Figure R1 has been included in the revised manuscript as Fig. 1 and Fig. R2 in the supplementary materials as Fig. S1. This point was clarified as well in Lines 96-104 in the revision:

"The stochastic sampling implicitly parameterized the uncertainties of the PBL and convection processes to a certain degree. As stated in Sun et al. (2021), using the sampled fluxes from a statistical distribution rather than the fluxes directly from individual PFTs can represent the mix of subgrid fluxes from horizontally mixed land cover types in reality. Moreover, the distribution of the sampled subgrid surface heat fluxes based on the assumed normal distribution resembles the distribution of realistic subgrid PFT heat fluxes within the grid cell in long-term statistics. As shown in Fig. 1 for the sensible heat flux, over the grid cells with 16 and 8 PFTs, the two distributions are highly consistent, in terms of mean value, variance and skewness. The latent heat flux has similar results (figure not shown). Given that those grid cells are stochastically selected and cover different climate regimes (Fig. S1), therefore, the assumed normal distribution works well and thus the sampled samples can represent the realistic features for climate simulation."

Comment 2:
As the manuscript reads now, it seems like the authors touched on a wide range of analysis of the atmospheric variables only briefly without really figuring out their scientific connections. Instead, the authors may consider restructuring the manuscript and dig deeper into aspects that are truly linked with the incorporation of the subgrid-scale treatment of surface heat fluxes. For example, the authors stated that the simulated large-scale circulation is significantly altered by the modified surface heat fluxes which further improves the simulated precipitation on the southern and eastern margins of TP. If so, is it possible to demonstrate the relationship between the changes in surface heat fluxes (Figs. 6&7) and the affected SLP field in Fig. 5? Also, it is very interesting to see the cloud feedbacks in EXP or EXP_COR, and that is supposed to be induced by the surface energy changes in this study. But in the context, the changes in cloud properties are considered the reason why surface heat fluxes are influenced.

Reply: Thanks for the valuable comments. The scientific connections among those variables (e.g., precipitation, surface energy fluxes, clouds and 2 m temperature) have been strengthened in the revision with a schematic diagram (Fig. R3) of figuring out

their physical links included. Also, the manuscript has been restructured accordingly, especially in Sect. 3.

Over eastern China and the eastern/southern borders of the TP, the changes in the PBL heating rate from EXP to EXP_COR (Fig. R4a&b) are analyzed to link the changes in surface heat fluxes with the affected SLP. The scientific connections between variables are disentangled as follows (Fig. R3a). As stated in Sun et al. (2021), in the EXP run, the subgrid variations of the land surface heat fluxes increase (decrease) the PBL heating rate over southern (northern) China. After taking the partitioning of subgrid surface heat fluxes into account, the increase (decrease) in the PBL heating rate over southern (northern) China is strengthened (Fig. R4b). Therefore, the destabilization (stabilization) in the lower atmosphere is further enhanced, promoting (suppressing) the development of local convection. Lower (higher) sea level pressure (SLP) anomalies over southern (northern) China are generated in the EXP_COR run than in the EXP run (Fig. R4g). In particular, compared with the EXP run, the anomalous high SLP over northern China slightly extends to the south and the anomalous low SLP over southern China retreats. The anomalous anticyclone over northern China expands accordingly, which engenders decreased precipitation on the eastern border of the TP and a slight dry bias over southern China. Convective precipitation dominates the changes of total precipitation over eastern China and the eastern margin of the TP. In the EXP_COR run, the easterly anomaly along 25° N-30° N partly blocks moisture transport from the ocean in the south to the southern margin of the TP, and therefore, the decrease of large-scale precipitation dominates the change of precipitation simulation on the southern margin of the TP.

As the reviewer indicated, we corrected the statement that the changes in clouds should be a result of the altered PBL heating rates and the associated local convection, although they in turn can affect the net surface heat fluxes. This is summarized in Fig. R3b.

In the revision, Figs. R3&4 are included as Figs. 14&6, respectively and the related edits are made in Lines 455-462:

"The causes are briefly summarized in Fig. 14a. The subgrid variations of the land surface heat fluxes increase (decrease) the PBL heating over southern (northern) China. With the further introduction of the partitioning of subgrid surface heat fluxes, the increase (decrease) in the PBL heating over southern (northern) China is elevated, thus destabilizing (stabilizing) the lower atmosphere. Resultantly, local convection is promoted (suppressed) over southern (northern) China. The changes of convective precipitation dominate the changes of total precipitation over eastern China and the eastern margin of the TP. The altered large-scale circulation associated with the easterly anomaly along 25° N-30° N partly blocks moisture transport from the ocean in the south to the southern margin of the TP. Accordingly, the decrease of large-scale precipitation is responsible for the reduced precipitation there."

and in Lines 463-467:

"The links among clouds, net surface shortwave flux and 2 m air temperature over eastern China are figured out in Fig. 14b. As the PBL heating decreases in northern China, the lower atmosphere stabilizes and local convection is suppressed. Accordingly, middle and high clouds, and associated CWP decrease (Figs. 9&10). Thus, SWCF decreases over northern China, which increases the net surface shortwave flux. As the surface gains more energy, the near-surface air temperature warms. In contrast, southern China features the opposite changes in the storyline."

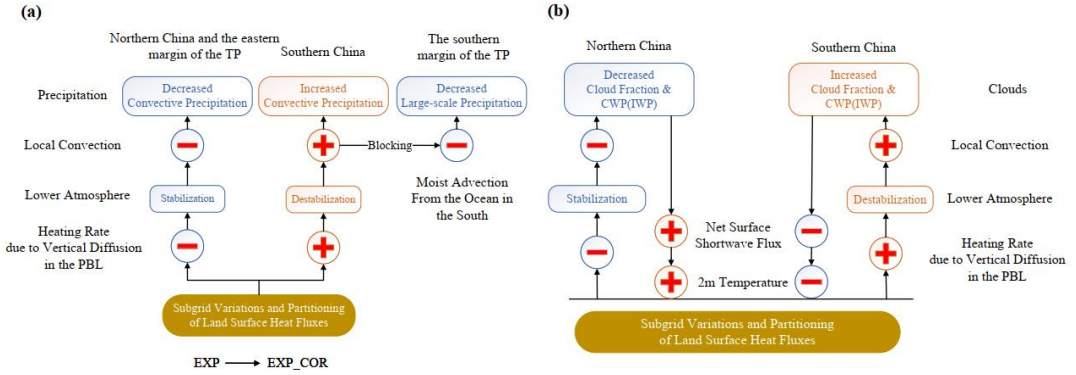

Figure R3. Schematic diagram of summarizing the climate impacts of parameterizing subgrid variations and partitioning of land surface heat fluxes to the atmosphere.

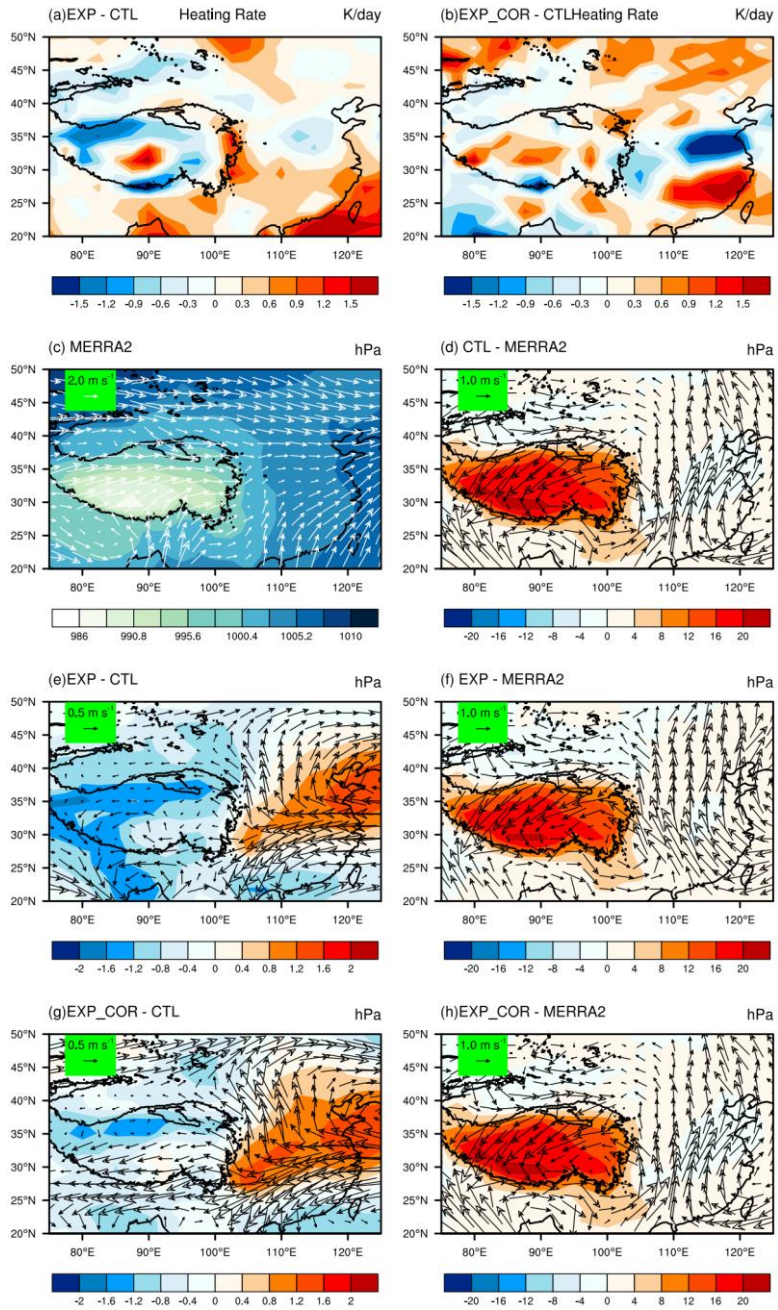

Figure R4. Spatial distributions of the differences of JJA-mean PBL heating (a) between EXP and CTL, and (b) between EXP_COR and CTL, JJA-mean SLP superposed by the vector $\vec{V}$ from (c) MERRA-2, and the differences (d) between CTL and MERRA-2, (e) between EXP and CTL, (f) between EXP and MERRA2, (g) between EXP_COR and CTL, and (h) between EXP_COR and MERRA2. The vector $\vec{V}$ is defined in Eq. (3).

Specific comments

Comment 1:

L75: Suggest changing the title to "Materials and methods" or "Methodology"

Reply: Done.

Comment 2:

L82: "all of the PFTs in the grid" -> "the corresponding grid"
Reply: Done.

Comment 3:
L88: "selected as N pairs" -> "paired with each other"
Reply: Done.

Comment 4:
L97: "normal distributions" see the general comment
Reply: Please see our response to the general comment 1.

Comment 5:
L152: "Sun et al. improved ... (Fig. 2c)" Should it be Fig. 2d or Fig. 2c? Fig. 2c is comparing Sun et al. results with the control case.

Reply: Sorry for this typo. It should be Fig. 2d (now Fig. 3d in the revision).

Comment 6:
L157: Given that the RMSE of EXP_COR is very close to EXP, is it sensitive to the average region the authors defined? Or, why do the authors choose 0-50°N, 0-180°E as the study area for the statistics?

Reply: Following reviewer #1's suggestion, Fig. 2 (now Fig.3) has been expanded to -48.5°S-48.5°N, -180°W-180°E to agree with the coverage area of the TRMM observations.

Comment 7:
L198-L200: If the authors can include the Fig.5b from Sun et al. (2021) into Fig. 5 in this manuscript, it may be easier for readers to understand the context on explaining model's overestimated precipitation in the southern TP.

Reply: Fig. 5a&b in Sun et al. (2021) has been included in the figure (now Fig. 6a&e in the revision).

Comment 8:
Figure 5: Does it show the moisture transport vector or wind speed? The unit as depicted in Fig. 5 is m s^{-1}.

Reply: This is the moisture transport vector ($\vec{\boldsymbol{V}}$) as shown in Eq. (2) (now Eq. (3) in the revision), which is given by $W^{-1}\int_{P_{top}}^{P_{bot}}(q\vec{u})dp/g$, representing the total horizontal moisture transport normalized to the column integrated moisture. Therefore, the unit is m s^{-1}. For clarity, we explained this more in Lines 227-229 in the revision:

"The vector $\vec{V}$ with the units of m s^{-1}, given by $W^{-1}\int_{P_{top}}^{P_{bot}}(q\vec{u})dp/g$, represents the total horizontal moisture transport normalized to the column-integrated moisture, where $\vec{u}$ is the horizontal wind vector."

and in Line 263:

"The vector $\vec{V}$ is defined in Eq. (3)."

Comment 9:
Figures 6-11: The inserted boxes do not zoom in much or indicate more useful information. They may be removed.
Reply: Done.

Comment 10:
L221: Remove "resulting in better agreement with the observations"
Reply: Done.

Comment 11:
L303-L305: This sentence is a little confusing. What is the difference between "subgrid variations in surface heat fluxes" and "their subgrid partitioning"? It might be good to provide an explanation.

Reply: The sentence has been rephrased in Lines 374-377 in the revision:

"The precipitation improvements over eastern China are mainly from the consideration of subgrid variations in surface heat fluxes (i.e., the EXP run where the sampled subgrid sensible and latent heat fluxes are stochastically paired with each other), while the improved precipitation simulations on the southern and eastern margins of the TP are attributed to the further inclusion of the partitioning of the subgrid surface heat fluxes (the EXP_COR run)."

Comment 12:
Figure 12: Could the authors make this blurry plotting of a higher quality?

Reply: Following review #1's suggestion, Fig.12 has been translated into Table 1 (Table R1 below) for clarity additionally with the seasonal statistics included.

Table R1. The COR and RMSE values in the CTL, EXP and EXP_COR runs. MAM is for March-April-May, JJA for June-July-August, SON for September-October-November, and DJF for December-January-February. The best performance among the three experiments is highlighted in bold.

Variables	Period	COR	RMSE

		CTL	EXP	EXP_COR	CTL	EXP	EXP_COR
Precipitation	MAM	**0.82**	**0.82**	0.81	**1.55**	**1.55**	1.61
	JJA	0.78	**0.80**	0.79	2.11	**2.03**	2.04
	SON	0.85	0.85	0.85	1.53	**1.52**	1.53
	DJF	**0.85**	0.84	0.84	**1.62**	1.65	1.73
	Annual	0.86	0.86	0.86	1.29	**1.27**	1.30
2 m Temperature	MAM	0.98	0.98	0.98	2.57	2.50	**2.49**
	JJA	0.95	0.95	0.95	2.70	**2.66**	2.67
	SON	0.98	0.98	0.98	2.64	19.94	**2.61**
	DJF	0.99	0.99	0.99	4.01	**3.76**	3.80
	Annual	0.98	0.98	0.98	2.50	5.86	**2.42**
Sensible Heat Flux	MAM	**0.67**	0.65	0.65	**34.08**	34.73	34.43
	JJA	0.55	**0.56**	**0.56**	30.67	**30.57**	30.89
	SON	0.86	0.86	0.86	**23.40**	25.79	23.92
	DJF	**0.88**	0.87	0.87	**23.71**	24.42	24.42
	Annual	**0.74**	0.73	0.73	**22.71**	23.72	23.28
Latent Heat Flux	MAM	**0.89**	0.88	0.88	**15.84**	16.37	16.23
	JJA	**0.82**	**0.82**	0.81	24.24	**23.18**	23.40
	SON	0.88	0.88	0.88	17.34	17.57	**17.33**
	DJF	**0.92**	0.91	0.92	**15.99**	16.93	16.44
	Annual	0.90	0.90	0.90	**13.92**	14.17	14.15
Net Surface Shortwave Flux	MAM	**0.92**	0.91	0.91	**21.89**	23.20	23.47
	JJA	0.83	0.83	0.83	**29.75**	29.84	30.21
	SON	0.96	0.96	0.96	**20.35**	26.06	21.10
	DJF	0.96	0.96	**0.97**	**24.28**	24.51	24.32
	Annual	0.93	0.93	0.93	**19.35**	21.04	20.05